Atmospheric neutrinos as a probe of eV^2-scale active-sterile oscillations

Raj Gandhi[*] and Pomita Ghoshal[†]

Harish-Chandra Research Institute, Chhatnag Road, Jhunsi, Allahabad 211019, India

(Received 7 February 2012; published 24 August 2012)

The downgoing atmospheric ν_μ and $\bar{\nu}_\mu$ fluxes can be significantly altered due to the presence of eV^2-scale active-sterile oscillations. We study the sensitivity of a large liquid argon detector and a large magnetized iron detector (like the proposed ICAL at INO) to these oscillations. Such oscillations are indicated by results from LSND, and more recently, from MiniBooNE and from reanalyses of reactor experiments following recent recalculations of reactor fluxes. There are other tentative indications of the presence of sterile states in both the ν and $\bar{\nu}$ sectors as well. Using the allowed sterile parameter ranges in a $3 + 1$ mixing framework in order to test these results, we perform a fit assuming active-sterile oscillations in both the muon neutrino and antineutrino sectors, and compute oscillation exclusion limits using atmospheric downgoing muon neutrino and antineutrino events. We find that (for both ν_μ and $\bar{\nu}_\mu$) a liquid argon detector, an ICAL-like detector or a combined analysis of both detectors with an exposure of 1 Mt/yr provides significant sensitivity to regions of parameter space in the range $0.1 < \Delta m^2 < 5$ eV^2 for $\sin^2 2\Theta_{\mu\mu} \geq 0.08$. Thus atmospheric neutrino experiments can provide complementary coverage in these regions, improving sensitivity limits in combination with bounds from other experiments on these parameters. We also analyze the bounds using muon antineutrino events only and compare them with the results from MiniBooNE.

DOI: 10.1103/PhysRevD.86.037301 PACS numbers: 14.60.Pq

I. INTRODUCTION AND MOTIVATION

Some significant recent experimental results in neutrino physics (MiniBooNE [1], reactor $\bar{\nu}_e$ flux recalculation [2,3], gallium data [4], CMB and big bang nucleosynthesis data [5–7]), along with the older LSND [8] result, have provided evidence of $\bar{\nu}_\mu \rightarrow \bar{\nu}_e$ oscillations at values of $L/E \approx 1$ m/MeV, where L is the baseline and E the neutrino energy. This has motivated the addition of one or more sterile antineutrino(s) with eV-scale mass(es) to the standard three-flavor scenario. While the experimental evidence remains intriguing, no clearly preferred theoretical model or framework has emerged so far.

These results have prompted a number of global analyses incorporating recent data as well as results from earlier experiments, which assume either a framework of three light active neutrinos and one $(3 + 1)$, or two $(3 + 2)$ sterile neutrinos [9–27].

Efforts to clarify the situation include plans to put in a new near detector or reusing the existing MiniBooNE detector at a near baseline [28]. There is also a proposal to use the Imaging Cosmic And Rare Underground Signals detector, a liquid argon time projection chamber at the CERN-PS to look for sterile neutrinos [29]. It has also been suggested that a large future liquid scintillator detector like NOνA or LENA be coupled with a compact decay-at-rest source at a short baseline in order to confirm or refute the signals of sterile neutrinos [30].

In this situation, it is useful to look at experiments which can provide data at *multiple* values of L and E, which would unambiguously signal the presence, or absence, of oscillations. It is also desirable to move to a class of experiment with backgrounds and uncertainties which are qualitatively different from those encountered in, for instance, MiniBooNE and LSND, or in reactors.

Motivated by these considerations, in this paper we study the role a large atmospheric detector can play in clarifying these issues. Two examples of such upcoming detectors are the proposed ICAL at INO [31] and a large liquid argon detector [32–34]. For simplicity, we consider the downgoing muon neutrino and muon antineutrino events in the energy range 1–20 GeV and baseline range 10–100 km. This provides a wide band of L/E with values that are relevant to the issues at hand. The lepton charge identification capability of such detectors, if magnetized, lends an edge by allowing discrimination between the neutrinos and antineutrinos, compared to a water Cerenkov detector like SuperKamiokande. It allows independent tests of the presence of sterile neutrinos in the muon and antimuon data samples, with higher statistical significance for the former due to the larger (by approximately a factor of 2) neutrino-nucleon charged current cross section.[1]

In the parameter range under study, strong sterile parameter constraints already exist from CDHS [35], CCFR [36], MINOS [18,37,38], SciBooNE/MiniBooNE [39] and SuperKamiokande atmospheric neutrino data

[*]raj@mri.ernet.in
[†]pomita.ghoshal@gmail.com

[1]It is not our intention here to assume that there is *CPT* violation, i.e., that ν and $\bar{\nu}$ oscillate differently. Our results below are based on a combined analysis of $\nu + \bar{\nu}$ events. Since the detectors in question can identify lepton charge effectively, we also provide results for $\bar{\nu}$ alone, for comparison with MiniBooNE and LSND, which see a signal predominantly in $\bar{\nu}$.

[9,40,41]. The present limits are summarized in Ref [16]. Recently, even stronger bounds from MINOS+ have been suggested in Ref [42], and the possibility of sterile neutrino information from atmospheric neutrino data in IceCube has been discussed in Ref [43]. Less stringent constraints also exist for the $\bar{\nu}_\mu$ sector from MiniBooNe [44,45]

In Sec. II, we motivate our study of sterile-scale oscillations using downgoing atmospheric muon neutrinos, and give the specifications of the two futuristic detectors we have analyzed for this purpose. Section III A gives our results for the exclusion limits from these detectors in the $\sin^2 2\Theta\mu\mu - \Delta m^2$ plane, comparing them with bounds obtained from the experiments listed above.

Since both LSND and MiniBooNE have provided evidence of eV^2 oscillations in the $\bar{\nu}_\mu$ sector, we separately investigate in Sec. III B the expected signal from $\bar{\nu}_\mu \to \nu_x$, utilizing the charge identification capability of such detectors, for a comparison with the bounds from MiniBooNE. Section IV summarizes our results and conclusions.

II. ATMOSPHERIC DOWNGOING MUON NEUTRINOS AND THE STERILE-SCALE OSCILLATION

Muon and electron neutrinos and antineutrinos produced in the earth's atmosphere provide a naturally occurring source of large fluxes spanning an extensive range of energies and baselines. While the upgoing electron and muon neutrinos with baselines of several thousands of kilometers pass through the earth, are influenced by earth matter effects and give good sensitivity to standard three-flavor neutrino oscillation parameters, the downgoing neutrinos have baselines of about 15–130 km. With an energy range between 1 and 20 GeV (above which fluxes become small), these neutrinos lie in the L/E range in which oscillations arising from the sterile mass-squared difference may be observed.

Assuming a 3 + 1 scheme (one nonstandard neutrino with a mass squared difference of $\Delta m^2(= \Delta m^2_{41}) \sim 1\ \mathrm{eV}^2$), the expressions for the relevant survival and oscillation probabilities with two-flavor sterile-scale oscillations are [14]

$$
\begin{aligned}
P_{\mu\mu} &= 1 - \sin^2 2\Theta_{\mu\mu} \sin^2[\Delta m^2 L/4E] \\
P_{e\mu} &= \sin^2 2\Theta_{e\mu} \sin^2[\Delta m^2 L/4E],
\end{aligned}
$$

where $\Theta_{\mu\mu}$ and $\Theta_{e\mu}$ are given by $\sin^2 2\Theta_{\mu\mu} = 4|U_{\mu4}|^2(1 - |U_{\mu4}|^2)$, $\sin^2 2\Theta_{e\mu} = 4|U_{e4}|^2|U_{\mu4}|^2$, and U is the 4×4 antineutrino mixing matrix. In the energy and baseline range corresponding to downgoing atmospheric neutrinos, the standard three-flavor oscillations are highly suppressed and one can perform the analysis using only two-flavor sterile-scale oscillations to a good approximation. From [17], we list the following best-fit values and 3σ ranges of these parameters:

$$
\begin{aligned}
&\sin^2 2\Theta^{bf}_{\mu\mu} = 0.083, \qquad 0.01 \le \sin^2 2\Theta_{\mu\mu} \le 0.25 \\
&\sin^2 2\Theta^{bf}_{e\mu} = 0.0023, \\
&4\times 10^{-4} \le \sin^2 2\Theta_{e\mu} \le 0.01 (\Delta m^2)^{bf} = 0.9\ \mathrm{eV}^2, \\
&0.7 \le \Delta m^2 \le 7\ \mathrm{eV}^2.
\end{aligned}
\tag{1}
$$

Here the superscript bf denotes the best-fit values.

We perform our statistical analysis using two kinds of proposed detectors:

(i) A large liquid argon detector, which can detect charged particles with very good resolution over the energy range of MeV to multi GeV, with magnetization over a 100-kT volume with a magnetic field of about 1 T [46]. We assume the following energy resolutions over the ranges relevant to our calculations [33]:

$$
\begin{aligned}
\sigma_{E_e} &= 0.01, \\
\sigma_{E_\mu} &= 0.01 \sigma_{E_{\rm had}} = \sqrt{(0.15)^2/E_{\rm had} + (0.03)^2}\, \sigma_{\theta_e} \\
&= 0.03\ \text{radians} = 1.72^o, \\
\sigma_{\theta_\mu} &= 0.04\ \text{radians} = 2.29^o \sigma_{\theta_{\rm had}} \\
&= 0.04\ \text{radians} = 2.29^o,
\end{aligned}
\tag{2}
$$

where E_e, E_μ and $E_{\rm had}$ are the lepton and hadron energies in GeV, σ_E are the energy resolutions and σ_θ are the angular resolutions of electrons, muons and hadrons as indicated. The energy resolution in terms of the neutrino energy is related to the leptonic and hadronic energy resolutions as follows:

$$
\sigma_\nu/E_\nu = \sqrt{(1-y)^2(\sigma_{\rm lep}/E_{\rm lep})^2 + y^2(\sigma_{\rm had}/E_{\rm had})^2}. \tag{3}
$$

Here the rapidity or the Bjorken scaling variable y is defined as $y = E_{\rm had}/E_\nu$, where $E_\nu = E_{\rm lep} + E_{\rm had}$ is the energy of the neutrino. The relation $E_\nu = E_{\rm lep} + E_{\rm had}$ is exact for quasielastic scattering and the closest analytic approximation for DIS scattering. Lepton-neutrino collinearity is assumed in this procedure, and is expected to hold true to a good approximation in the multi-GeV neutrino energy range. Hence the energy resolution in terms of the neutrino energy is given by

$$
\sigma_{E_\nu} = \sqrt{(0.01)^2 + (0.15)^2/yE_\nu + (0.03)^2} \tag{4}
$$

for both electron and muon neutrinos. In our computation, we take the average rapidity in the GeV energy region to be 0.45 for neutrinos and 0.3 for antineutrinos [47]. These average rapidity values have been verified to be accurate using realistic hadron event simulations. The angular resolution of the detector for neutrinos can be worked out to be

$\sigma_{\theta_{\nu e}} = 2.8^o$, $\sigma_{\theta_{\nu\mu}} = 3.2^o$. The energy threshold and ranges in which charge identification is feasible are $E_{\rm threshold} = 800$ MeV for muons and $E_{\rm electron} =$ 1–5 GeV for electrons.

(ii) An iron calorimeter detector like ICAL, which, like the above detector, offers the advantage of muon charge discrimination using magnetization with a field of 1.3 T, allowing a separate observation of atmospheric muon neutrino and antineutrino events. For this detector, standard resolutions of 10° in angle and 15% in energy are assumed.

The muon event rates are a function of both $P_{\mu\mu}$ and $P_{e\mu}$, but $P_{e\mu}$ is highly suppressed due to the smallness of the parameter $\sin^2 2\Theta_{e\mu}$. Thus the downgoing muon event spectrum reflects the behavior of $P_{\mu\mu}$ and shows signatures of the sterile parameters $\Theta_{\mu\mu}$ and Δm^2. In Fig. 1, the downgoing muon neutrino distribution with and without two-flavor sterile oscillations is shown as a function of the neutrino energies, integrated over $\cos\theta_z$ bins.

We assume a 1 Mt/yr exposure for both types of detectors, standard detector resolutions as above, and flux uncertainties and systematic errors incorporated by the pull method [48]. The values of uncertainties are chosen as in Ref [49]: flux normalization error 20%, flux tilt factor, zenith angle dependence uncertainty 5%, overall cross-section uncertainty 10%, overall systematic uncertainty 5%. We take a double binning in neutrino energy and zenith angle in the energy range 1–20 GeV and $\cos\theta_z$ range 0.1–1.0. To be consistent with the detector resolution, the bin widths are required to be $\geq$ the resolution widths. For the above neutrino energy and zenith angle ranges, this allows us to take 20 energy bins and 18 angle bins for these values of resolution width. The atmospheric fluxes are taken from the three-dimensional calculation in Ref [50]. We have taken into account the neutrino production height distribution in the atmosphere [51].

III. EXCLUSION LIMITS WITH STERILE OSCILLATIONS IN THE ν_μ AND $\bar{\nu}_\mu$ EVENT SPECTRA

One can extract the statistical sensitivity with which experimental setups like the ones described above may be able to constrain sterile parameters using the downgoing muon and antimuon event spectra as the signal. We perform this study in two stages:

(a) The best exclusion limits possible from this analysis are determined using simultaneously the downgoing ν_μ and $\bar{\nu}_\mu$ event spectra for both kinds of detectors and doing a combined fit.

(b) In order to test the MiniBooNE/LSND antineutrino results, the atmospheric downgoing $\bar{\nu}_\mu$ event spectra with sterile oscillations for both kinds of detectors are analyzed to determine the sterile parameter bounds, and compared with the bounds from MiniBooNE.

A. Limits with a combined ν_μ, $\bar{\nu}_\mu$ analysis

For this study, the sterile oscillation exclusion limits are computed by combining both the atmospheric downgoing muon and antimuon event spectra with sterile-scale oscillations. This involves taking (i) the "expected" spectrum $N_{\rm th}$, in which sterile oscillations are included, and (ii) the "observed" spectrum $N_{\rm ex}({\rm no}-{\rm osc})$, where "no-osc" indicates no sterile-scale oscillations. Since we expect no differences in the oscillations of neutrinos c ompared to antineutrinos in the 3 + 1 model when matter effects are absent, we have assumed equal probabilities for them for downgoing events. The exclusion limits are

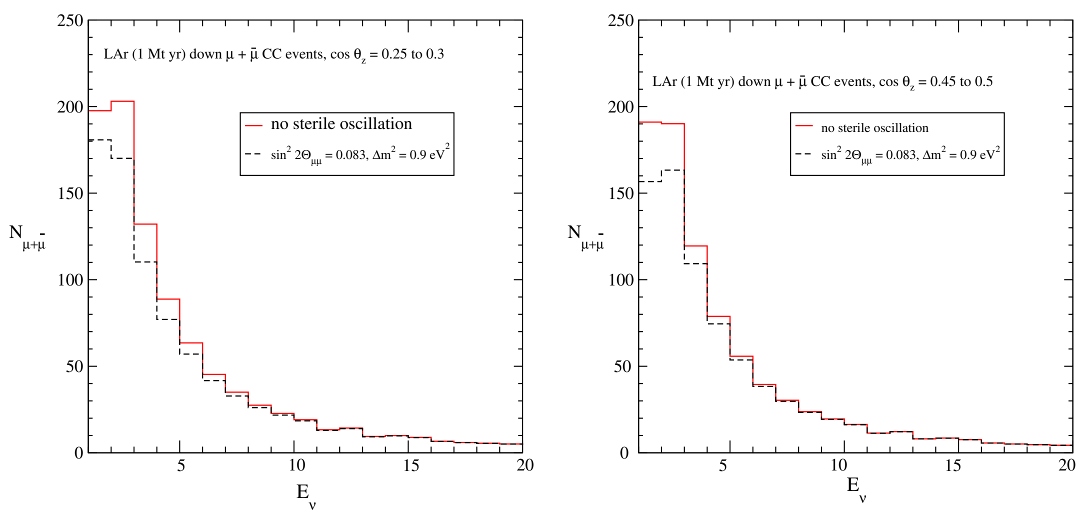

FIG. 1 (color online). LAr downgoing $\mu + \bar{\mu}$ event spectrum vs neutrino energy integrated over the two specific $\cos\theta_z$ bins with and without two-flavor sterile-scale oscillations, using best-fit sterile parameter values.

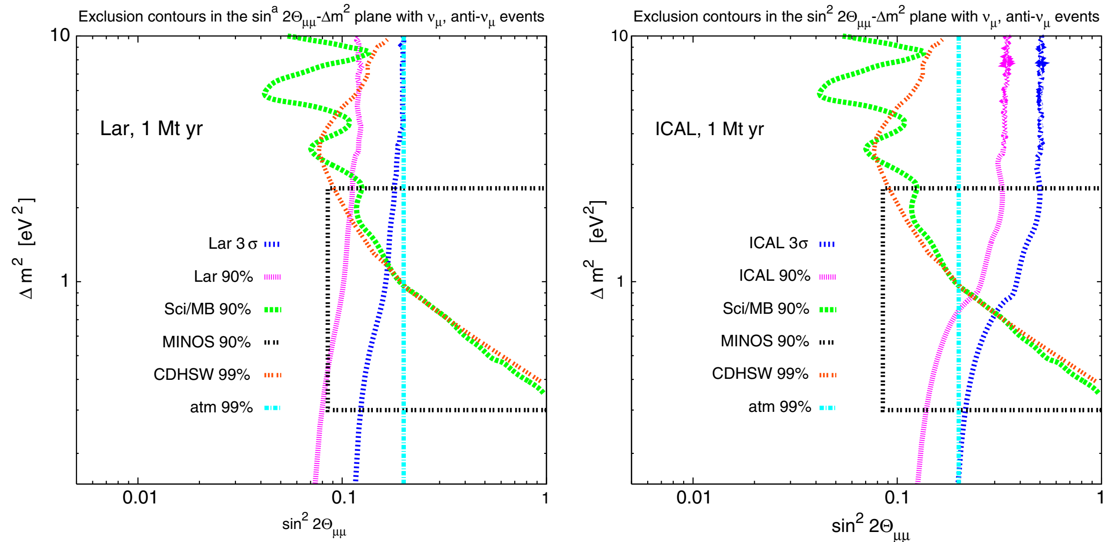

(a) (b)

FIG. 2 (color online). Exclusion curves using (a) liquid argon and (b) ICAL downgoing muon and antimuon events with sterile oscillations—Comparison with 99% confidence level (c.l.) limit from atmospheric analysis [9,16], 90% limits from SciBooNE/MiniBooNE [39] and MINOS [37], 99% c.l. limit from CDHSW [16,35].

presented in Fig. 2 for a liquid argon detector and an ICAL detector, with an exposure of 1 Mt/yr for both. Figure 3 shows the results from a combined analysis of ICAL + liquid argon. The bounds obtained from our analysis are compared with the 99% exclusion region from atmospheric neutrino data [9,16], the 90% limits from SciBooNE/MiniBooNE [39] and MINOS [37] and the 99% limit from the CDHSW disappearance analysis [16,35].

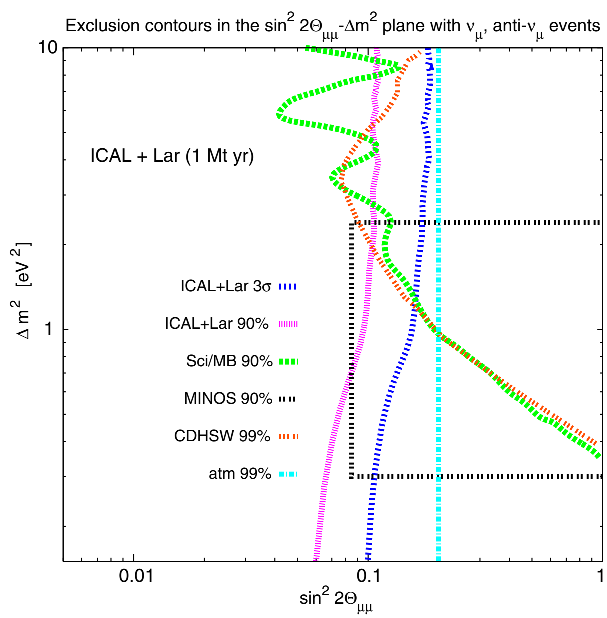

FIG. 3 (color online). Same as Fig. 2 using ICAL + liquid argon downgoing muon and antimuon events.

With a liquid argon detector and an exposure of 1 Mt/yr, regions greater than $\sin^2 2\Theta_{\mu\mu} \sim 0.09$ can be excluded at 90% c.l. with a combination of muon and antimuon events over most of the allowed Δm^2 range. An ICAL-like detector with a similar exposure gives a weaker 90% c.l. exclusion bound at $\sin^2 2\Theta_{\mu\mu} \sim 0.15$. A combined analysis of the two experiments gives a 3σ exclusion bound for $\sin^2 2\Theta_{\mu\mu} \geq 0.11$, and a 90% c.l. limit for $\sin^2 2\Theta_{\mu\mu} \geq 0.08$, which is seen to be an improvement over the earlier bounds obtained from atmospheric neutrinos, as well as those from CDHSW, SciBooNE/MiniBooNE and MINOS, over significant regions of the parameter space. Note that the sensitivity using this setup is better in the low Δm^2 region ($\Delta m^2 < 1$ eV^2), part of which lies outside the present global fit range, but our purpose here is to demonstrate that such an experiment is capable of providing significant bounds over the entire parameter space which can contribute to constraining sterile parameters in combination with other experiments in a future global analysis.

B. Testing LSND and Miniboone results with sterile oscillations in the $\bar{\nu}$ sector

Here we compute the sterile oscillation exclusion limits using the downgoing antimuon event spectrum for comparison with the results from MiniBooNE/LSND antineutrino data. The bounds obtained from this analysis are presented in Fig. 4. The left and right panels correspond to the exclusion bounds for the parameters $\Delta\bar{m}^2$ and $\sin^2 2\bar{\Theta}$ with the downgoing $\bar{\nu}_\mu$ spectrum for an ICAL detector and a liquid argon detector respectively, both with an exposure of 1 Mt/yr. Here $\Delta\bar{m}^2$ and $\bar{\Theta}_{\mu\mu}$ denote

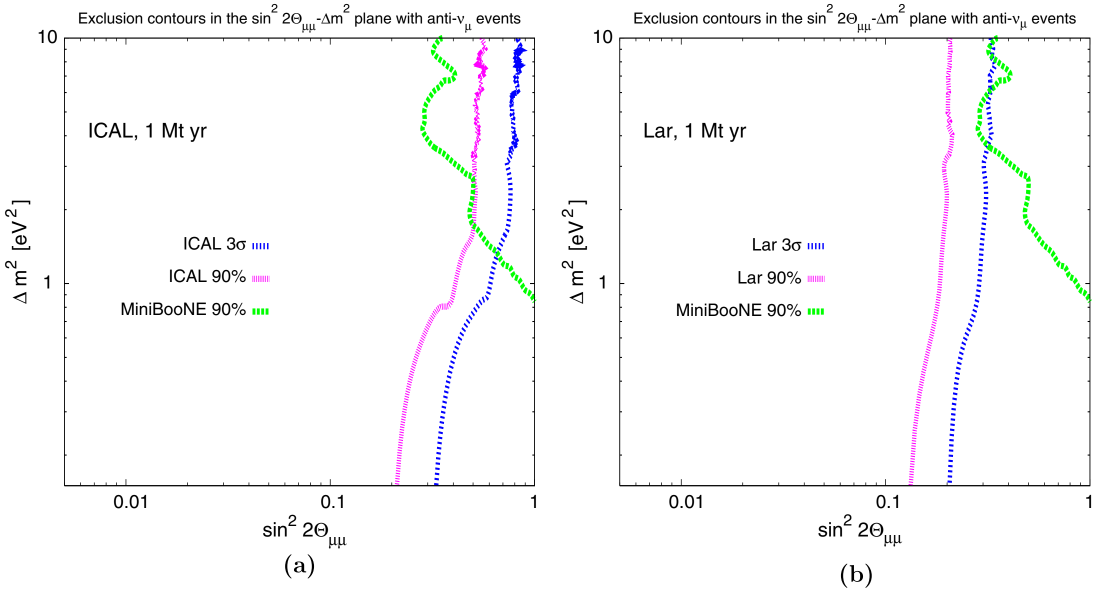

FIG. 4 (color online). Exclusion curves using (a) ICAL and (b) liquid argon downgoing antimuon events with sterile oscillations–Comparison with 90% exclusion limit from MiniBooNE [45] antineutrino analysis.

the mixing parameters for antineutrinos. The 90% exclusion limit from MiniBooNE [45] is superimposed on both figures. It can be seen that this setup provides a 90% c.l. exclusion capacity with an ICAL-like detector with an exposure of 1 Mt/yr for about $\sin^2 2\bar{\Theta}_{\mu\mu} > 0.4$ for a range $0.1 < \Delta\bar{m}^2 < 5$ eV^2, and for a liquid argon detector with an exposure of 1 Mt/yr for about $\sin^2 2\bar{\Theta}_{\mu\mu} > 0.15$ for a range $0.1 < \Delta\bar{m}^2 < 5$ eV^2. Thus a liquid argon detector gives stronger bounds than those from the MiniBooNE antineutrino analysis.

IV. SUMMARY

In this paper, we have studied the possible sensitivity of atmospheric neutrino data in a large magnetized iron calorimeter detector like the proposed ICAL at INO and a large liquid argon detector, to eV^2-scale active-sterile oscillations. Such detectors are capable of distinguishing lepton charge and hence discriminating between neutrino and antineutrino events. With the present sterile parameter ranges in a 3 + 1 mixing framework, downgoing atmospheric ν_μ and $\bar{\nu}_\mu$ events can show signatures of eV^2-scale oscillations, due to their suitable energy and baseline range (neutrinos with multi-GeV energies and baselines ranging from about 10–100 km). Our analysis has been done in two parts:

(I) To be consistent with homogeneity in $\nu - \bar{\nu}$ behavior in the 3 + 1 scenario, we assumed identical active-sterile oscillations in both the muon neutrino and antineutrino sectors and derived active-sterile oscillation exclusion limits (Figs. 2 and 3), comparing them with the limits obtained from Refs [9,16,17,35,37,39].

(a) With a liquid argon detector (1 Mt/yr), regions greater than $\sin^2 2\Theta_{\mu\mu} \sim 0.09$ can be excluded at 90% c.l. with a combination of muon and antimuon events, over most of the Δm^2 range. A 3σ exclusion bound is possible for $\sin^2 2\Theta_{\mu\mu} \sim 0.13$.

(b) With an ICAL detector (1 Mt/yr), a weaker 90% c.l. exclusion bound is obtained at $\sin^2 2\Theta_{\mu\mu} \sim 0.15$ with a combination of muon and antimuon events.

(c) With a combined analysis of ICAL (1 Mt/yr) and liquid argon (1 Mt/yr), a 90% c.l. exclusion limit is obtained for $\sin^2 2\Theta_{\mu\mu} \geq 0.08$ and a 3σ bound for $\sin^2 2\Theta_{\mu\mu} \geq 0.11$, which compares favorably with present limits from CDHSW, MINOS, MiniBooNE and atmospheric neutrinos.

(II) For testing the predictions of LSND and MiniBooNE, we performed a fit with active-sterile oscillations in the muon antineutrino sector, comparing the results with the exclusion limits from MiniBooNE (Fig. 4), and derived the following 90% c.l. exclusion bounds:

(a) an ICAL-like detector with an exposure of 1 Mt/yr for about $\sin^2 2\bar{\Theta}_{\mu\mu} > 0.4$ for a range $0.1 < \Delta\bar{m}^2 < 5$ eV^2,

(b) a liquid argon detector with an exposure of 1 Mt/yr for about $\sin^2 2\bar{\Theta}_{\mu\mu} > 0.15$ for a range $0.1 < \Delta\bar{m}^2 < 5$ eV^2.

The limits for both detectors from an exposure of 1 Mt/yr may be accessible in a time frame of about 10–15 years.

In conclusion, a downgoing event analysis using large future atmospheric detectors may be helpful in providing significant complementary constraints on the sterile parameters, which can strengthen existing bounds when combined with other experimental signatures of sterile-scale oscillations. Such a setup exhibits better sterile oscillation sensitivity in the low Δm^2 region ($\Delta m^2 < 1\ \mathrm{eV}^2$). Evidence (or the lack of it) from such detectors has the advantage of originating in a sector which is different from those currently providing clues pointing to the existence of sterile neutrinos (i.e., short-baseline experiments). Additionally, it permits access to a wide-band of L/E, which is important if oscillatory behavior is to be unambiguously tested.

ACKNOWLEDGMENTS

We acknowledge long-standing collaborations on INO/ICAL physics with Srubabati Goswami and S. Uma Sankar, which have informed this work. R. G. would like to acknowledge the hospitality of the CERN Theory Division, where this work was initiated. He is also grateful for financial support from the DAE XI Plan Neutrino project. P. G. thanks S. T. Petcov for useful discussions. This work was supported in part by the INFN program on "Astroparticle Physics" (P. G.).

[1] A. A. Aguilar-Arevalo *et al.* (MiniBooNE Collaboration), Phys. Rev. Lett. **105**, 181801 (2010).
[2] T. A. Mueller *et al.*, Phys. Rev. C **83**, 054615 (2011).
[3] P. Huber, Phys. Rev. C **84**, 024617 (2011); **85**, 029901(E) (2012).
[4] For a discussion and analysis, see C. Giunti and M. Laveder, Phys. Rev. C **83**, 065504 (2011) and references therein.
[5] M. C. Gonzalez-Garcia, M. Maltoni, and J. Salvado, J. High Energy Phys. 08 (2010) 117.
[6] J. Hamann, S. Hannestad, G. G. Raffelt, I. Tamborra, and Y. Y. Y. Wong, Phys. Rev. Lett. **105**, 181301 (2010).
[7] E. Giusarma, M. Corsi, M. Archidiacono, R. de Putter, A. Melchiorri, O. Mena, and S. Pandolfi, Phys. Rev. D **83**, 115023 (2011).
[8] A. Aguilar *et al.* (LSND Collaboration), Phys. Rev. D **64**, 112007 (2001).
[9] M. Maltoni and T. Schwetz, Phys. Rev. D **76**, 093005 (2007).
[10] G. Karagiorgi, Z. Djurcic, J. M. Conrad, M. H. Shaevitz, and M. Sorel, Phys. Rev. D **80**, 073001 (2009).
[11] E. Akhmedov and T. Schwetz, J. High Energy Phys. 10 (2010) 115.
[12] J. Kopp, M. Maltoni, and T. Schwetz, Phys. Rev. Lett. **107**, 091801 (2011).
[13] C. Giunti and M. Laveder, Nucl. Phys. B, Proc. Suppl. **217**, 193 (2011).
[14] C. Giunti and M. Laveder, Phys. Rev. D **83**, 053006 (2011).
[15] C. Giunti, arXiv:1106.4479.
[16] C. Giunti and M. Laveder, Phys. Rev. D **84**, 073008 (2011).
[17] C. Giunti and M. Laveder, Phys. Lett. B **706**, 200 (2011).
[18] C. Giunti and M. Laveder, Phys. Rev. D **84**, 093006 (2011).
[19] O. L. G. Peres and A. Y. Smirnov, Nucl. Phys. **B599**, 3 (2001).
[20] A. Strumia, Phys. Lett. B **539**, 91 (2002).
[21] W. Grimus and T. Schwetz, Eur. Phys. J. C **20**, 1 (2001).
[22] M. Maltoni, T. Schwetz, and J. W. F. Valle, Phys. Lett. B **518**, 252 (2001).
[23] A. Palazzo, Phys. Rev. D **83**, 113013 (2011).
[24] M. C. Gonzalez-Garcia, M. Maltoni, and C. Pena-Garay, Phys. Rev. D **64**, 093001 (2001).
[25] G. L. Fogli, E. Lisi, and A. Marrone, Phys. Rev. D **63**, 053008 (2001).
[26] G. Karagiorgi, Z. Djurcic, J. M. Conrad, M. H. Shaevitz, and M. Sorel, Phys. Rev. D **80**, 073001 (2009); **81**, 039902 (E) (2010).
[27] M. C. Gonzalez-Garcia and C. Pena-Garay, Phys. Rev. D **63**, 073013 (2001).
[28] For details, see the talk by G. Mills at the Short Baseline Neutrino Workshop, Fermilab, 2011, https://indico.fnal.gov/conferenceTimeTable.py?confId=4157#20110512.
[29] F. Pietropaolo, talk at the Short Baseline Neutrino Workshop, Fermilab, 2011, https://indico.fnal.gov/conferenceTimeTable.py?confId=4157#20110512.
[30] S. K. Agarwalla, J. M. Conrad and M. H. Shaevitz, J. High Energy Phys. 12 (2011) 085.
[31] INO Collaboration, http://www.imsc.res.in/~ino/OpenReports/report.html.
[32] A. Rubbia, arXiv:hep-ph/0402110.
[33] A. Bueno, A. J. Melgarejo, S. Navas, Z. Dai, Y. Ge, M. Laffranchi, A. Meregaglia, and A. Rubbia, J. High Energy Phys. 04 (2007) 041.
[34] D. B. Cline, F. Raffaelli, and F. Sergiampietri, JINST **1**, T09001 (2006).
[35] F. Dydak *et al.*, Phys. Lett. **134B**, 281 (1984).
[36] I. E. Stockdale *et al.*, Phys. Rev. Lett. **52**, 1384 (1984).
[37] P. Adamson *et al.* (MINOS Collaboration), Phys. Rev. Lett. **107**, 011802 2011); Also see the talk by M. Shaevitz at PANIC 11, July 26 2011, at http://web.mit.edu/panic11/talks/monday/plenary.html.
[38] D. Hernandez and A. Y. Smirnov, Phys. Lett. B **706**, 360 (2012).
[39] K. B. M. Mahn *et al.* (SciBooNE and MiniBooNE Collaborations), Phys. Rev. D **85**, 032007 (2012).
[40] S. M. Bilenky, C. Giunti, W. Grimus, and T. Schwetz, Phys. Rev. D **60**, 073007 (1999).
[41] M. Maltoni, T. Schwetz, and J. W. F. Valle, Phys. Lett. B **518**, 252 (2001).
[42] A. Sousa on behalf of the (MINOS Collaboration), arXiv:1110.3455.
[43] V. Barger, Y. Gao, and D. Marfatia, Phys. Rev. D **85**, 011302 (2012).

[44] A. A. Aguilar-Arevalo *et al.*, Phys. Rev. Lett. **98**, 231801 (2007).
[45] A. A. Aguilar-Arevalo *et al.* (MiniBooNE Collaboration), Phys. Rev. Lett. **103**, 061802 (2009).
[46] A. Ereditato and A. Rubbia, Nucl. Phys. B, Proc. Suppl. **155**, 233 (2006).
[47] R. Gandhi, C. Quigg, M. H. Reno, and I. Sarcevic, Astropart. Phys. **5**, 81 (1996).
[48] M. C. Gonzalez-Garcia and M. Maltoni, Phys. Rev. D **70**, 033010 (2004).
[49] R. Gandhi, P. Ghoshal, S. Goswami, P. Mehta, S. U. Sankar, and S. Shalgar, Phys. Rev. D **76**, 073012 (2007).
[50] M. Honda, T. Kajita, K. Kasahara, and S. Midorikawa, Phys. Rev. D **70**, 043008 (2004).
[51] T. K. Gaisser and T. Stanev, Phys. Rev. D **57**, 1977 (1998).